Excitation of Kinetic Geodesic Acoustic Modes by Drift Waves in Nonuniform Plasmas

Z. Qiu[1], L. Chen[1,2] and F. Zonca[3,1]

[1]*Inst. Fusion Theory & Simulation and Dept. of Physics, Zhejiang Univ., Hangzhou, P.R.C.*
[2]*Dept. Physics & Astronomy, University of California, Irvine CA 92697-4575, U.S.A.*
[3]*Associazione Euratom-ENEA sulla Fusione, C.P. 65 - I-00044 - Frascati, Italy*

Geodesic Acoustic Modes (GAM) [1, 2] correspond to finite-frequency zonal structures unique in toroidal plasmas, which are capable of scattering microscopic drift-wave-type turbulence (DW) including drift Alfvén waves into stable short radial-wavelength regime [2], and, thereby, regulating the turbulence intensity and the associated wave-induced transports. Besides this wave-wave interaction process, resonant wave-particle interactions with energetic particles, i.e., the so called energetic particle induced GAM (EGAM), has also attracted much research interest [3, 4, 5]. Effect of energetic particles on the nonlinear interactions between DW and GAM has also been discussed [5, 6]. In this work, we show that the nonlinear physics of GAM, including both wave-wave and wave-particle nonlinearities, can be described by a unified theoretical framework; which can be applied, in various limits, to study the nonlinear dynamics of the GAM, DW and EP system, such as nonlinear self-regulation of DW via GAM excitation, and EGAM nonlinear saturation due to wave-particle trapping.

I. Unified theoretical framework of GAM

The nonlinear GAM equations including both wave-wave and wave-particle nonlinearities are derived from nonlinear gyrokinetic theory (equation (3) of Ref. [7]),

$$\omega_d D_d A_d = (c/B_0)(T_i/T_e)k_\theta A_d \partial_r A_G, \tag{1}$$

$$\omega_G \varepsilon_{EGAM} A_G = (\alpha/2)(c/B_0)\rho_i^2 k_\theta \partial_r \left(A_d \partial_r^2 A_d^* - c.c.\right), \tag{2}$$

in which, subscripts d and G denote DW and GAM, respectively, $\alpha = 1 + \delta P_\perp/(en_0\delta\phi_P)$ with $\delta P_\perp$ being the perturbed perpendicular pressure, A is the radial envelope; and $-i\partial_r \equiv k_r = nq'\theta_k$ represents the radial envelope wave vector. D_d and ε_{EGAM} are, respectively, the linear dielectric functions of DW and EGAM, with the detailed expressions given in [7] and [4]. Here, we give the expression of ε_{EGAM} explicitly; which is important for our discussion,

$$\varepsilon_{EGAM} = \varepsilon_{GAM} + 2\pi B\overline{\delta\phi_G}e^{i\omega_G t}\frac{\Omega_i^2}{n_c k_r^2}\sum_{\sigma=\pm1}\int \frac{EdEd\Lambda}{|v_\parallel|}\frac{\partial F_{0h}}{\partial E}\frac{\omega_{dh}^2}{\omega^2-\omega_{tr}^2}.$$

ε_{GAM} is the linear GAM dielectric function accounting for the thermal plasma response [2].

We note that, in ε_{EGAM}, the EP drive term is formally linear, while the EP equilibrium distribution function obeys the following renormalized nonlinear equation

$$-i\bar{\omega}\hat{F}_{0h} = i\frac{e^2\hat{\omega}_d}{16}|\delta\phi_G(\tau)|^2\frac{\partial}{\partial E}\left[\frac{\hat{\omega}_d(\bar{\omega}-i\gamma)}{(\bar{\omega}-i\gamma)^2-(\omega_{0r}^2-\omega_{tr})^2}\right]\frac{\partial}{\partial E}\hat{F}_{0h}(\bar{\omega}-2i\gamma)+F_{0h}(0). \tag{3}$$

Here, $\bar{\omega}$ denotes the slow time scale for F_{0h} evolution from its initial value $F_{0h}(0)$, $\hat{F}_{0h}$ is the Laplace transform of F_{0h}, and $|\gamma| \ll \omega_{0r}$ is the growth rate of $\delta\phi_G$. Equation (3) is of the form

of a Dyson equation, and describes the evolution of F_{0h}, due to emission and reabsorption of EGAM. Note that, in deriving equation (3), only evolution in E needs to be taken into account [9], since both P_ϕ and μ are conserved.

This set of equations, i.e., equations (1), (2) and (3), describe the fully nonlinear evolution of the GAM, DW and EP system, with multiple spatial scales due to system nonuniformities; such as GAM continuum, DW nonuniformity, and EP radial profile [8]; and, thus, generally require numerical solution. However, it becomes analytically tractable in some simplified limits. Here, we will examine two such limits. In the first example, we will neglect the effects of DW, and study the nonlinear saturation of EGAM. In the second limit, we will neglect effects of EPs, and study nonlinear interactions between GAM and DW.

II. Nonlinear EGAM saturation due to wave-particle trapping

Nonlinear evolution of EGAM can be studied in the absence of DW. The linear theory of EGAM [4] can be recovered neglecting the nonlinear evolution of F_{0h}. Here, we focus on the nonlinear saturation of EGAM due to wave-particle trapping, which has previously been discussed in [9]. Here, we will use a different approach and investigate the properties of the EP phase space structures.

For resonant EPs, we have in equation (3), $\omega_{0r} - \omega_{tr} \simeq -(\partial\omega_{tr}/\partial E|_{E_r})(E - E_r)$ and $\hat{\omega}_d = \hat{\omega}_d(E_r)$. Let's further neglect sources and sinks, and assume weak drive; i.e., $|\gamma| \ll |\bar{\omega}|$. The Dyson equation, equation (3), describing nonlinear EGAM evolution then becomes

$$\hat{F}_{0h} = \beta\partial_E \left(1/(\bar{\omega}^2 - \alpha^2(E-E_r)^2)\right)\partial_E \hat{F}_{0h} + (i/\bar{\omega})F_{0h}(0);$$

where, $\alpha = \partial\omega_{tr}/\partial E|_{E_r}$ and $\beta = e^2\hat{\omega}_d^2|\delta\phi_\tau|^2/(16)$. Taking $\xi = E - E_r$, and $\Psi = (1/(\bar{\omega}^2 - \alpha^2\xi^2))\partial_\xi \hat{F}_{0h}$, the Dyson equation for $\hat{F}_{0h}$ reduces to

$$\left(\partial_\xi^2 + \bar{\omega}^2/\beta - \alpha^2\xi^2/\beta\right)\Psi = (i/(2\pi\bar{\omega}))\partial_{xi}F_{0h}. \tag{4}$$

The homogeneous equation can be written as Weber's equation, and describes phase space structure Ψ (or $\hat{F}_{0h}$) formation in the resonant particle frame. The "eigenmode" dispersion relation in ξ or E, is then $\bar{\omega}^2 = \beta\kappa^2$, with κ defined as $\kappa^4 = \alpha^2/\beta$. We then have $|\bar{\omega}^2| \sim \partial\omega_{tr}/\partial E|_{E_r}\hat{\omega}_d|\delta\phi|$; i.e., typical for wave-particle trapping ($\bar{\omega} \sim \sqrt{\delta\phi}$) [9].

III. Nonlinear interactions between GAM and DW in nonuniform plasmas

Neglecting the contribution of EPs, equations (1) and (2) describe the nonlinear interactions between DW turbulence and self-generated GAM. We note that, the fully nonlinear two-field equations, derived without separating DW into a fix-amplitude pump and a lower sideband with much smaller amplitude, contain all the major nonlinear effects, and can be applied to investigate the nonlinear saturation and turbulence spreading of DW turbulence due to GAM excitation. Finite group velocities associated with kinetic dispersiveness and system nonuniformities, such as GAM continuum and nonuniformity of diamagnetic drift frequency are self-consistently taken into account, and could modify the parametric instability qualitatively.

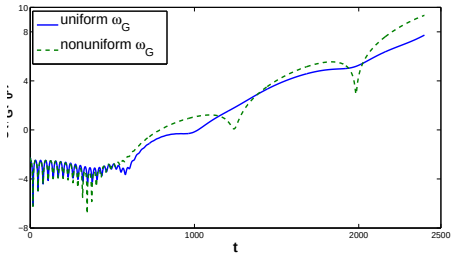

Figure 1: Logarithm of A_G v.s. t for nonuniform $\omega_*(r)$ and pump.

A. Nonlinear excitation of GAM by DW in nonuniform plasmas

In this subsection, we focus on the absolute/convective nature of the parametric instability, while the nonlinear saturation of DW will be discussed in the next subsection. Following [7] and separating the DW into a pump wave and a lower sideband with a much smaller amplitude, we recover the normalized coupled nonlinear equations of GAM and DW sideband [7]:

$$\left(\partial_t + i\omega_P - i\omega_*(r) - iC_d\omega_*\rho_i^2\partial_r^2\right)A_S = \Gamma_0^*\hat{A}_G, \quad (5)$$

$$\left(\partial_t^2 + \omega_G^2(r) - C_G\omega_G^2(r_0)\rho_i^2\partial_r^2\right)\hat{A}_G = -\Gamma_0\partial_t\partial_r^2 A_S. \quad (6)$$

Here, ω_P is the real frequency of the pump DW, C_d and C_G are $O(1)$ coefficients; representing the finite kinetic dispersiveness due to finite radial envelope variations and $\hat{A}_G = \partial_r\delta\phi_G/\alpha$ with $\alpha = i(\alpha_i\omega_P T_e/T_i)^{1/2}$. Γ_0 is the normalized radial envelope of DW pump that has a radial scale length $L_P \propto \sqrt{\rho_i L_d}$ from solving linear DW eigenmode equation, with a profile of $\omega_*(r) = \omega_*(1-(r-r_0)^2/L_d^2)$. There are three spatial scales in this problem; i.e., GAM continuum L_G, L_P, and L_d with $L_d \propto \sqrt{\rho_i L_d} \ll L_d \sim L_G \sim a$. The problem can be then solved order by order, taking advantage of the scale separation.

On the short time scale, we may consider only a localized pump, and ignore the effects of GAM continuum and $\omega_*(r)$ nonuniformities. The convective/absolute nature of the parametric instability is then determined by the linear group velocities of GAM and DW sideband. For typical tokamak parameters, with $C_dC_G > 0$, we then have $V_dV_G > 0$, i.e., DW sideband and GAM satisfying frequency and wavenumber matching conditions propagate in the same direction, and the parametric instability is a convective amplification process, which is of less interest for fusion research. The generated GAM and DW sideband are coupled together and propagate out of the unstable region and, thus, can not effectively modulate DW. For cases with $C_G < 0$ [2], we have $V_dV_G < 0$, and the parametric process is an absolute instability. In the rest of this section, we will focus on the more typical case with $C_G > 0$.

Next, we consider the longer time scale, and take the nonuniformity of $\omega_*(r)$ into account, while we neglect the contribution of GAM continuum in order to delineate the effect of nonuniform $\omega_*(r)$. Equations (6) and (5) are solved numerically, and the result shows that coupled DW sideband and GAM wave packet are reflected at the turning points of DW induced by $\omega_*(r)$ nonuniformity, and are amplified as they propagate through their original position r_0 again. The convective instability, as a result, becomes a quasi-exponentially growing absolute instability.

Finally, with all the nonuniformities self-consistently included, the coupled nonlinear equations (5) and (6), are solved numerically. The time histories of GAM amplitude at $r = r_0$ is

shown in Fig. 1, in which the solid curve corresponds to the nonuniform GAM frequency case, while the dashed line illustrates the uniform GAM frequency case for comparison. One notes, that the two cases are qualitatively similar, i.e., the nonuniformity of $\omega_*(r)$ is the dominant effect on the longer time scale, which renders the initially convective parametric instability into a quasi-exponentially growing absolute instability on a longer time scale. On the other hand, GAM continuum plays a relatively minor role here. Due to the frequency mismatch induced by spatially varying $\omega_G(r)$, the case with nonuniform $\omega_G(r)$ has a slightly different growth rate.

B. Nonlinear saturation of DW due to GAM excitation

In this subsection, we study the nonlinear saturation of DW due to GAM excitation by numerically solving equations (1) and (2), without separating DW into pump and sideband. For the simplicity of discussion, we ignore linear drives and dampings of DW and GAM, and study the nonlinear evolution of a given DW envelope solved self-consistently from linear eigenmode equation with nonuniform $\omega_*(r)$. Following the discussion of previous section, we ignore the contribution of GAM continuum and focus on the $C_dC_G > 0$ case. $C_d = 1$ is fixed, and two parameters, i.e., the amplitude of DW ($A_d(t=0)$) and C_G are varied. We found that, the excitation of GAM is determined by the competition between the nonlinear drive (parameterized by $A_d(t=0)$) and the dispersiveness due to linear group velocities (parameterized by C_G).

The mode structure at $t = 500$ is shown in Fig. 2, where the dotted curve is the DW amplitude at $t = 0$, dashed and dotted-dashed curves are respectively the real and imaginary part of A_d at $t = 500$, and the solid curve is A_G at $t = 500$. One notes that, at $t = 500$, GAM generation is maximized at $r \simeq \pm 25$, where the gradient of A_d is maximized, and DW turbulence spreads due to generation of GAM. The energy of DW and GAM are qualitatively represented by $\int dr|A_d|^2$ and $\int dr|A_G|^2$, and their changes with time are shown in Fig. 3. The increase of $\int dr|A_G|^2$, is shown to be consistent with the decrease of $\int dr|A_d|^2$. DW is saturated at $t > 700$.

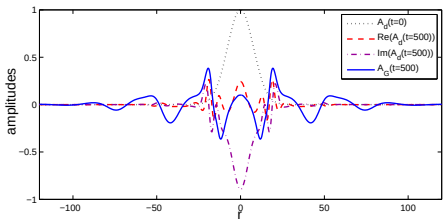

Figure 2: mode structures at $t = 500$

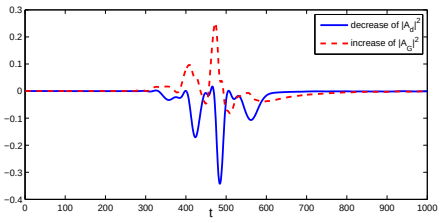

Figure 3: energy exchange between DW and GAM

References

[1] N. Winsor, J. L. Johnson, and J. M. Dawson, Phys. Fluids 11, 2448 (1968).
[2] F. Zonca and L. Chen, Europhys. Lett. 83, 35001 (2008).
[3] G. Fu, Phys. Rev. Lett. **101** (2008) 185002.
[4] Z. Qiu, F. Zonca and L. Chen, Plasma Phys. Control. Fusion 52, 095003 (2010).
[5] D. Zarzoso, Y. Sarazin, X. Garbet,et al, Phys. Rev. Lett. 110, 125002 (2013).
[6] R. Dumont, D. Zarzoso, Y. Sarazin, et al, Plasma Phys. Control. Fusion 55, 124012 (2013).
[7] Z. Qiu, L. Chen and F. Zonca, Phys. Plasmas 21, 022304 (2014).
[8] Z. Qiu, F. Zonca, and L. Chen, Physics of Plasmas 19, 082507 (2012).
[9] Z. Qiu, F. Zonca and L. Chen, Plasma Sci. Tech. 13, 257 (2011).